ACADEMIA ROMÂNĂ
Revue Roumaine de Chimie
https://www.icf.ro/rrch/

Rev. Roum. Chim.,
2024, *69*(3–4), 171–182
DOI: 10.33224/rrch.2024.69.3-4.07

SUSTAINABILITY APPROACH TO CORROSION MITIGATION USING ECO-FRIENDLY INHIBITOR FOR OIL AND GAS APPLICATIONS

Idawu Yakubu SULEIMAN,[a,c,*] Kabiru MU'AZU,[b] Omah Augustine DINOBI,[a]
Egoigwe Vincent SOCHIMA[d] and Njoku Romanus EGWUONWU[a]

[a]Department of Metallurgical and Materials Engineering, University of Nigeria, Nsukka, Nigeria
[b]Department of Pilot Plant and Fabrication, National Research Institute for Chemical Technology, Zaria, Nigeria
[c]African Centre of Excellence for Sustainable Power and Energy Development (ACE-SPED) University of Nigeria, Nsukka
[d]Department of Electronic Engineering, University of Nigeria, Nsukka, Nigeria

Received October 15, 2023

Investigation of *Euphorbia hirta leaves* as green corrosion inhibitor for mild steel in 0.5 M hydrochloric acid using gravimetric and potentiodynamic polarization techniques was carried out. Characterization carried out on the leaves were quantitative, qualitative analyses, Fourier Transform Infrared Spectroscopy (FT-IR), and Gas Chromatography-Mass Spectrometry (GC-MS). Scanning electron microscopy (SEM) attached with electron dispersive spectroscopy (EDS) was used to characterize the Substrates before and after corrosion tests. Both the inhibitor concentration, time, and temperature were varied accordingly. The corrosion rate increased with an increase in temperature and decreased with increases in both inhibitor concentrations and time.

An inhibition efficiency of 98.32% recorded at the optimum concentration of 12 g/L. Phytochemical results revealed tannins, alkaloids, saponins, and flavonoids with their contents. FT-IR and GC–MS revealed some functional groups such as Aliphatic cyanide/nitrile, C=N, Primary amine, CN stretch, Aliphatic bromo compounds, C-Br stretch, 7,17 Hexadecadienal, etc which were responsible for the protection of mild steel in the acidic medium. The inhibition efficiency obtained suggested the effectiveness of the inhibitor and acted as a mixed-type inhibitor. The substrates without green inhibitors were rough with severe pits, while the surfaces with optimum green inhibitors were protected. The results obtained from weight loss, and polarization were in good agreement with each other. Green corrosion inhibitors can, therefore, serve as an alternative to synthetic. The inhibition efficiency obtained is well above the minimum acceptable limit of 70% required of a good inhibitor. It can be used in the formulation of paints for coating of pipes in oil and gas industries.

INTRODUCTION

Sustainability in corrosion mitigation for oil and gas applications involves adopting eco-friendly practices and using environmentally benign inhibitors to protect metal surfaces from corrosion.[1] Deterioration of materials is a significant problem in the oil and gas industries, leading to equipment degradation, safety risks, and environmental pollution. Implementing a

* Corresponding author: idawu.suleiman@unn.edu.ng / +2348036057915

sustainable approach to corrosion prevention can minimize the negative impact on the environment while maintaining the integrity and longevity of the assets.[1,2]

Engineering materials are not stable in natural and industrial environments and are always liable to corrosion in hostile environments.[2,3] Instead of traditional, toxic, and hazardous inhibitors such as borates, chromates, and phosphates are used as anti-corrosion inhibitors for materials in any media.[4] The focus is on sustainability by selecting eco-friendly inhibitors that are derived from renewable resources, natural compounds, biodegradable, and pose minimal risk to human health and the environment.[4,5] The inhibitors must also be low in toxicity to aquatic life and other organisms, reducing their impact on ecosystems in case of accidental leakage and renewables.[5]

However, the inhibition actions of the inhibitors are attributed to their interactions with the metal surface via physical or chemical adsorption processes, which take place through the replacement of water molecules by organic inhibitor molecules from the metal surface.[6] Previous works shown that the adsorption of an inhibitor on a metal surface depends on the nature, surface charge of the metal, adsorption mode, its chemical structure, and the type of the electrolyte solution.[7,8]

Another work carried out by [9] also agreed that organic compounds containing hetero-atoms such as phosphorus (P), nitrogen (N), sulfur (S), and oxygen (O) with high electron density as well as those containing multiple bonds are effective corrosion inhibitors. All plant products are organic in nature and their constituents such as tannins, organic and amino acids, saponins, alkaloids, flavonoids, glycosides, and pigments are known to exhibit inhibiting action.[10–17] Acid solutions are widely used in oil and gas industries such as acid cleaning, acid descaling, acid pickling, and oil well acidizing which require the use of corrosion inhibitors to restrain their corrosion attack on metallic materials in the industries.[18]

Therefore, in continuation of our interests in the sustainability approach to corrosion mitigation using eco-friendly inhibitors for oil and gas applications in acidic environments has been investigated using weight loss and potentiodynamic polarization techniques. Characterizations of the leaf extract by X-ray fluorescent (XRF), Fourier Transforms Infrared Spectroscopy (FT-IR) and Gas Chromatography–Mass Spectrometry (GC–MS) and Scanning electron microscope/energy dispersive spectroscopy (SEM/EDS) on the material surface before and after film formation using the technique were also carried out. Among the studied leaves is *Euphobia Hirtal (EH)* exhibited good efficiency in inhibition corrosion in various aggressive media. The sustainability of corrosion inhibition was, therefore, proposed for this research.

MATERIALS AND METHODS

Materials preparation

Mild steel used for this study was obtained from Steel Company in Lagos State, Nigeria. The chemical composition of mild steel used for weight loss and potentiodynamic polarization was determined by X-ray fluorescence (XRF) and the results are presented in Table 1.

Table 1

Chemical composition of mild steel

Element	Fe	C	Si	Mn	P	S	Co	Mo	Ni	Al	Cu
% Wi	99.01	0.170	0.033	0.434	0.016	0.014	0.05	0.014	0.18	0.002	0.015

Inhibitor preparation

One kilogram of *Euphobia* leaves presented in Fig. 1 was obtained from the farm land, Nsukka Nigeria. Cleaning, and drying of the leaves at room temperature for three days were carried out. Dried leaves were then ground into fine powder using a mortar and pestle. About five hundred grams (500 gm) of ground sample was then extracted in 1.5 L of 70 % ethanol and 30 % distilled water was used as solvent using the maceration method by separating funnel. The extract and the final stage of collecting the liquid at 110 °C before evaporation was used. The concentration of the stock solution was expressed in terms of gram per litre (g/L) and the concentration of 3–18 g/L of the extract was prepared according to the work of.[19]

Fig. 1 – *Euphorbia Hirtal* leaf.

Preparation of solution

Preparation of 0.5 M HCl was prepared by diluting of analytical grade with double distilled water. *Euphobia hirtal* extract was dissolved in the acid solution at the required concentrations (g/L). The solution in the absence of an inhibitor was taken as blank (0) for comparison purposes.[19] The test solutions were freshly prepared before each experiment by adding *Euphobia Hirtal (EH)* extract directly to the corrosive solution. Concentrations of *Euphobia Hirtal (EH)* extract used were: 0, 3, 69, 12, 15, and 18 g/L respectively. Experiments were performed in triplicate to ensure good results.

Determination of phytoconstituents of the leaf extract

The phytoconstituents of the leaves were determined by quantitative and qualitative methods. The analyses were carried out at the Multi-Users Laboratory, Ahmadu Bello University, Zaria, Nigeria. Figures 2 and 3 presented the results respectively.

Preparation of specimens

Mild steel sheets were cut into triangular shapes of 20 mm by 10 mm with the following chemical compositions shown in Table 1. The specimens were polished with emery papers of 400–1600 grades and subsequently decreased and stored in the desiccators to avoid re-oxidation. The weight of the samples was taken before and after the weight loss carried out by.[20]

Weight loss measurements

Already-weighed specimens were separately immersed in 1000 millilitres (mL) of 0.5 M HCl solutions containing control (0), 3, 6, 9, 12, 15, and 18 g/L of *EH* extract for the periods of day 1, day 2, day 3, day 4, day 5, day 6, and day 7 respectively. After the elapsed periods, specimens were taken out, washed, dried, and reweighed. All the experiments were performed in triplicate, and average values were recorded. The experiment was carried out at different temperatures of 30, 45, and 60 °C respectively. From the measured weight loss data, the corrosion rate (mpy) and the inhibition efficiency (IE) were calculated using equations 1 and 2.[21–22]

Corrosion rate

$$(\text{mpy}) = \frac{534W}{DAT} \quad (1)$$

where W, D, A, and T will be in units of milligrams, grams per cubic centimetre, square inches, and hours, respectively. The inhibition efficiency (IE %) and surface coverage (θ) were calculated from equation 3:

Inhibition efficiency

$$(\text{IE }\%) = \frac{CRa}{CRp} x \frac{100}{1} \quad (2)$$

Surface coverage

$$(\theta) = \frac{CRa - CRp}{CRa} \quad (3)$$

Electrochemical measurements

The specimens were embedded in epoxy resin leaving a working area of 1.33 cm^2. The working surface was subsequently ground with 600 and 1800-grit grinding papers and cleaned with distilled water and ethanol. The solutions (0.5 M HCl) were prepared from an analytical reagent. Potentiodynamic polarization measurements were done using an Autolab potentiostat (PGSTAT30 computer-controlled) with the General-Purpose Electrochemical Software (GPES) package version 4.9. Anodic and cathodic polarization curves were

obtained with a scan rate of 2 mv/s in the potential range from –0.2 mv to –0.8 mv relative to the corrosion potential (E_{corr}). Values of the corrosion current density (i_{corr}) were obtained by extrapolation of the cathodic branch of the polarization curve back to E_{corr}. The Tafel slopes, corrosion potential, and corrosion current were calculated using a Frequency Response Analyzer (FRA). All the tests were performed at temperature of 30 °C. The inhibitor efficiency was calculated from Eq. 3 according to[22–24]

$$IE\ \% = \frac{i_{corr} - i'_{corr}}{i_{corr}}\ x\ 100\% \quad (4)$$

where i_{corr} and are the corrosion current densities of mild steel in the absence and presence of the inhibitor respectively. The parameters used for this method are presented in Table 2.

Table 2

Parameters used in the potentiodynamic electrochemical technique at 35 ºC

Parameters	Material
Initial voltage (V) Wrt OCP	–1.5
Final voltage (V) Wrt OCP	1.5
Scan rate (mV/s)	0.01

Fourier transforms infrared spectrophotometer (FT-IR)

The extract was characterized by using Fourier Transforms Infrared Spectroscopy (FT-IR) method for the identification of hydroxyl, aromatic hydrocarbon, chemical bonding and functional groups. The FT-IR was carried out using the Perkin Elmer 2000 Model at the Energy Centre, University of Nigeria, Nsukka. The spectra were recorded and the interpretations were done using Standard Library.[6,27]

Gas Chromatograph–Mass Spectrometry (GC–MS) Analysis

About 1 mL of each concentration of the extract was analyzed by GC–MS using QP 2010 Plus Shimadzu product equipped with two fused-silica capillary columns (60 m 9 0.22 mm), and film thickness at the National Research Institute for Chemical Technology, Zaria.

Characterization of the coupons

The mild steel surface was prepared for SEM and EDX studies by keeping the specimens for an hour in the electrolyte with and without the optimum concentrations of the inhibitor. The mild steel specimens were then washed with distilled water dried and analyzed using SEM/EDX. A Philips model XL30SFEG scanning electron microscope with an energy-dispersive X-ray analyzer attached was used for surface analysis.[30–32]

RESULTS AND DISCUSSION

Phytoconstituents of the *Euphobia Hirtal (EH)* extract

The detailed results of phytochemical constituents carried out on the extract by both quantitative and qualitative analyses showed that *Euphobia Hirtal (EH)* contains Saponins, Tannins, Alkaloids, Flavonoids, Glycosides, and Volatile oil. Tables 3 and 4 presented the quantitative and qualitative analyses of *Euphobia Hirtal (EH)* extract respectively. From the results, the constituents can be adsorbed onto the metallic surface by blocking the active corrosion site or reducing the evolution of hydrogen gas at the cathode. This may be attributed to the fact that some of these phytoconstituents contain heteroatoms such as O, N, S, P, and both aromatic and functional groups. This agrees with earlier research reported.[12]

Table 3

The qualitative analysis of *Euphobia Hirtal (EH) leaf* extract

Euphobia Hirtal (EH) leaf	Tannins	Saponins	Flavonoids	Glycosides	Alkaloids	Volatile oil
	+	+	–	+	+	+

Table 4

The quantitative analysis of *Euphobia Hirtal (EH) leaf* extract

Euphobia Hirtal (EH) leaf	Tannins (%)	Saponins (%)	Flavonoids (%)	Glycosides (%)	Alkaloids (%)	Volatile oil (%)
	15.10±0.01	3.23±0.03	0.000	0.65±0.12	1.34±0.03	0.65±0.24

Fourier Transforms Infrared (FT-IR) Spectroscopy results

Figures 2 and 3 show the IR absorption spectra and their functional groups. The prominent peaks obtained from the FT-IR spectroscopy for the *Euphorbia Hirtal (EH)* extract were presented in Table 5 and it also confirms the previous works of.[18,28] The inhibitor showed an effective anticorrosion potential and the results indicated that the inhibition mechanism involved blockage of the mild steel by inhibitor molecules via adsorption. In general, the phenomenon of adsorption was influenced by the nature and surface charge of the metal, by the type of aggressive electrolyte, and by the chemical structure of inhibitors.[22]

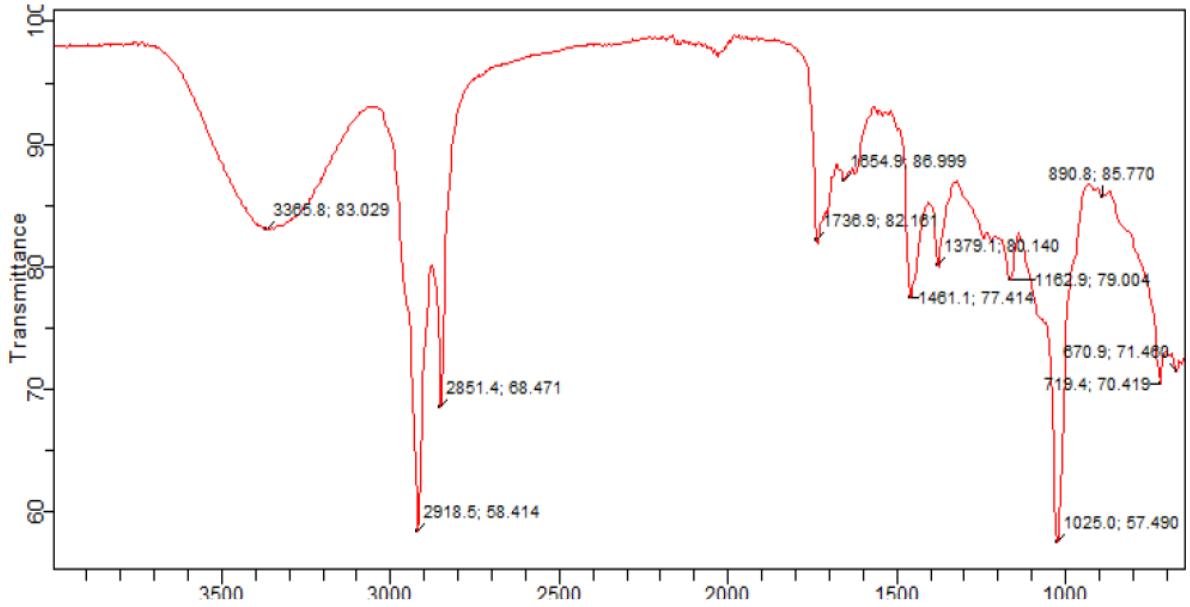

Fig. 2 – IR absorption spectrum of *Euphorbia Hirtal* leaf extract.

Table 5

Prominent peaks obtained from reflectance FTIR spectroscopy *Euphorbia Hirtal (EH)* extract

S/No.	Frequency range (cm^{-1})	Band Assignments
1.	3365.8	Aliphatic primary amine, NH_2 stretch
2.	2158.4	Aliphatic cyanide/nitrile, C=N
3.	2918.5	Methyne C_nH_{2n+2} stretch
4.	854.9	Five membered ring anhydrides
5.	1756.9	Alkyl carbonate
6.	1379.1	Phenol or tertiary, OH bend
7.	1461.1	Methylene C-H bend
8.	1162.9	Organic sulphates
9.	890.8	Vinylidene C-H out of plate bend
10.	719.4	Methylene – (CH_2) n-rocking {n>3}
11.	690.9	Aliphatic bromo compounds, C-Br stretch
12.	102.5	Primary amine, CN stretch

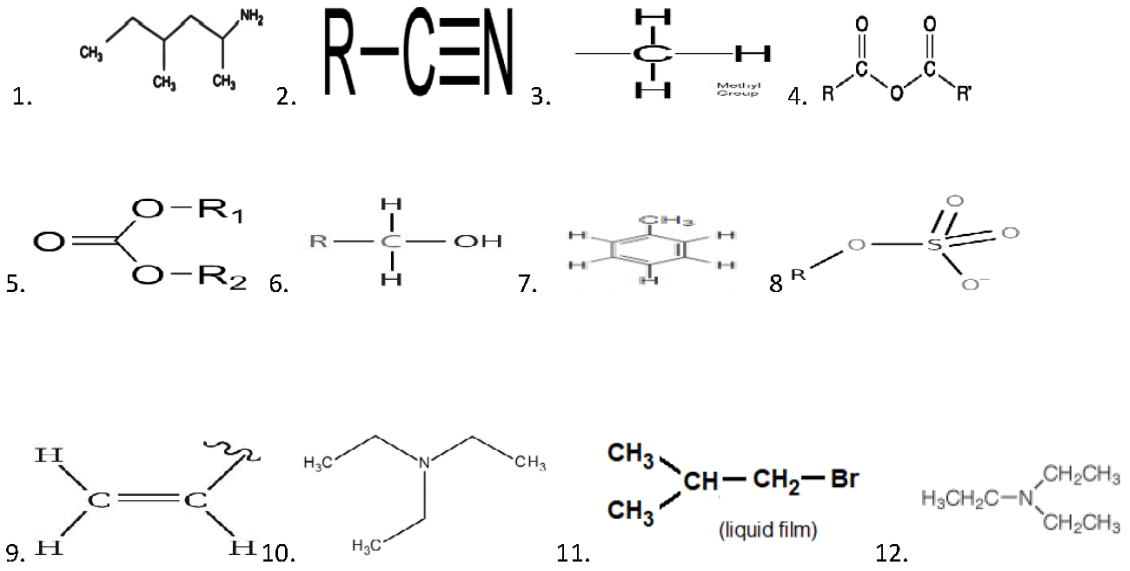

Fig. 3 – Chemical bonds/Functional groups of IR Absorption Spectrum of *Euphorbia Hirtal (EH)*.

Gas Chromatography-Mass Spectrometry (GC-MS) Analysis

GC–MS analysis data obtained from the *Euphorbia Hirtal (EH)* extract compounds identified in the ethanol distillate were presented in Table 6 and Fig. 4 presented the GC-MS spectra. The table revealed the presence of 9,17 Octadecadienal, 7,17 Hexadecadienal, and so on. The revealed functional groups are good corrosion inhibitors as reported by.[6,7] The extract contains oxygen atoms, hydroxyl, aromatic rings, and hydrocarbon which are the centres of adsorption. However, adsorption involving organic molecules at the metal solution interface may occur in any of the following ways: (*i*) the electrolytic attraction between the charged molecule and the charged metal; (*ii*) interaction of unshared electron pairs in the molecules with the metal; (*iii*) interaction of s electrons with metal; (*iv*) combination of the above findings.[18]

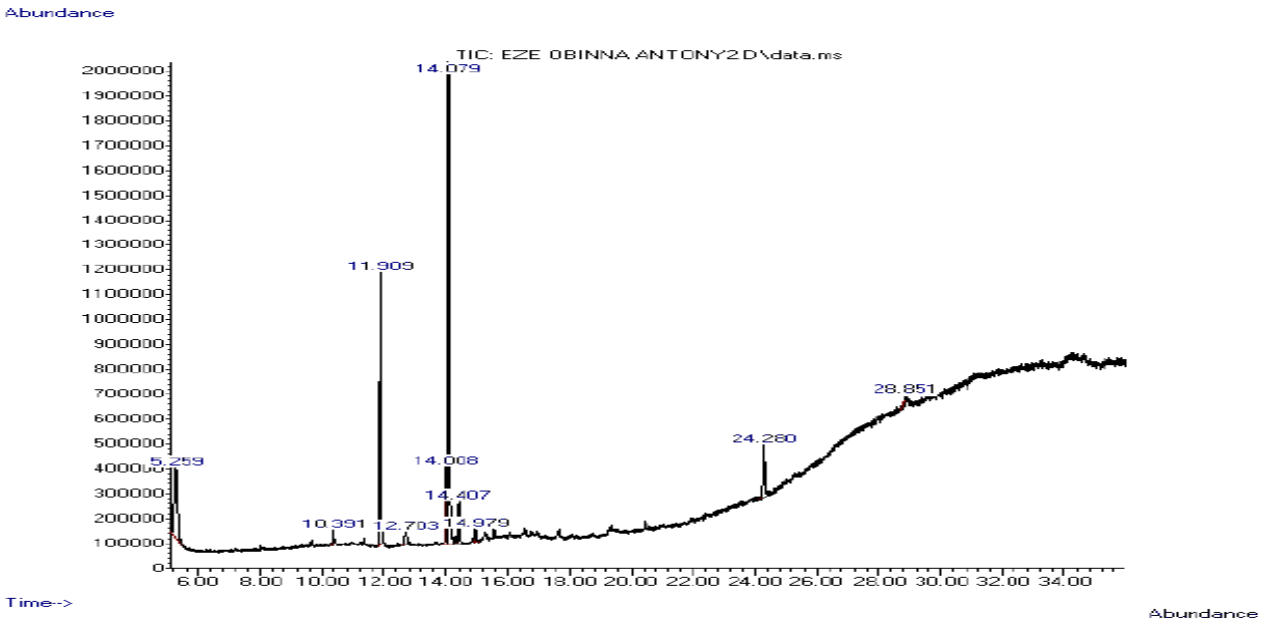

Fig. 4 – GC-MS analysis results (chemical compounds identified in the ethanol distillate of *Euphorbia Hirtal*).

Table 6

The chemical compounds identified in the ethanol distillate of (*EH*) extract by GC-MS

Pk#	RT	Area %	Library/ID	Ref#	Molecular Formula	Molecular weight g/mol
1	5.259	15.62D	9,17-Octadecadienal, 9,12-Octadecadienoic acid, 7,11-Hexadecadienal	125003 140137, 98680	$C_{18}H_{32}O$ $C_{18}H_{32}O_2$ $C_{16}H_{28}O$	264 280 236
2	10.391	0.74 D	Cyclohexadecane, 9-Eicosene, 5-Eicosene	87836, 140276, 140275	$C_{16}H_{32}$ $C_{20}H_{40}$ $C_{20}H_{40}$	224 280 280
3	11.909	19.26D	Hexadecanoic acid, methyl ester, Hexadecanoic acid, methyl ester, Hexadecanoic acid, methyl ester	130820, 130813, 130822	$C_{17}H_{34}O_2$ $C_{17}H_{34}O_2$ $C_{17}H_{34}O_2$	270 270 270
4	12.703	1.99 D	cis-Vaccenic acid, Oleic Acid, Hexadecanoic acid, ethyl ester	142073 142071 144304	$C_{18}H_{34}O_2$ $C_{18}H_{34}O_2$ $C_{18}H_{36}O_2$	282 282 284
5	14.008	6.00 D	11,14-Octadecadienoic acid, methyl ester, 9,15-Octadecadienoic acid, methyl ester, Methyl 10-trans,12-cis-octadecadie noate	153884 153899 153874	$C_{19}H_{34}O_2$ $C_{19}H_{24}O_2$ $C_{19}H_{34}O_2$	294 294 292
6	14.079	44.37 D	9-Octadecenoic acid, methyl ester, 9-Octadecenoic acid, methyl este	155754, 155721	$C_{19}H_{36}O_2$ $C_{19}H_{36}O_2$	296 296
7	14.407	3.67 D	Methyl stearate, Heptadecanoic acid, 16-methyl-, methyl ester, Methyl stearate	157881 157956 157885	$C_{19}H_{38}O_2$ C19H38O $C_{19}H_{38}O_2$	298 298 298
8	14.979	1.38 D	7,10,13-Hexadecatrienoic acid, methyl ester, 7,10,13-Hexadecatrienoic acid, methyl ester, Cyclododecyne	124916 124917 35042	$C_{16}H_{26}O_2$ $C_{16}H_{26}O_2$ $C_{12}H_{20}$	250 250 164
9	24.280	6.15 D	Squalene, Squalene, 5,9,13-Pentadecatrien-2-one,6,10,1-4-trimethyl	243219 243217 123157	$C_{30}H_{50}$ $C_{30}H_{50}$ $C_{18}H_{30}O$	410 410 262
10	28.814	0.35 D	Methyl (25RS)-3. beta. -hydroxy-cholesten-26-oate, erythro-9,10-Dibromopentacosane, Rhodopin	250932 267311 271155	$(C_{27}H_{44})_3$ $C_{25}H_5Br_2$ $C_{40}H_{58}O$	1104 465 554
11	28.851	0.48 D	Cholest-4-ene, 3. beta. -hoxy)-, Methyl(25RS)-3. beta. -hydroxy-5-cholesten-26-oate, 9-Octadecene, 1-[3-(octadecyloxy)propoxy]-	250967 250932 272301	$C_{29}H_{52}O_2$ $C_{27}H_{42}O_4$ $C_{39}H_{78}O_2$	432 430 578

Effect of *Euphorbia hirta extract* on mild steel

Weight loss measurements were performed on mild steel immersed in 0.5 M HCl solutions with and without (*EH*) extract for seven (7) days. The results obtained in the absence and the presence of the inhibitor at various concentrations are presented in Fig. 5. It can be seen that inhibition efficiency increases with the increase in inhibitor concentrations, which could be due to the increase in the mass and charge transfer to the mild steel surface leading to the adsorption of inhibitor molecules and reduction in the metal dissolution as shown in the extract characterizations by both FT-IR and GC-MS spectroscopies. Further increase in the inhibitor concentration causes little or negligible change and the highest inhibition efficiency occurred at the optimum concentration of the inhibitor (12 g/L). Owing to the acidity of the corrosive medium, the extract that contains the phytochemical constituents, functional groups from both the FT-IR and GC-MS respectively could not remain in the solution in its free base state and may exist as neutral species or in its cationic form which were presented in table 6 respectively. This assertion also agrees with the findings of the previous studies.[17,18] The high inhibition efficiency recorded could be possibly because Cl^{-1} was hydrated in HCl and this can be poorly adsorbed onto the metal surface leaving more active sites for the adsorption of the inhibitor-neutral species – and thus inhibition efficiency increased with increased concentrations of the inhibitor in HCl medium. Hence, it can be concluded that while adding the inhibitor to the HCl solution anions like $C_{25}H_5Br_2$, and OH are present in the inhibitor solution, and the unshared pair of electrons is present.[19,20]

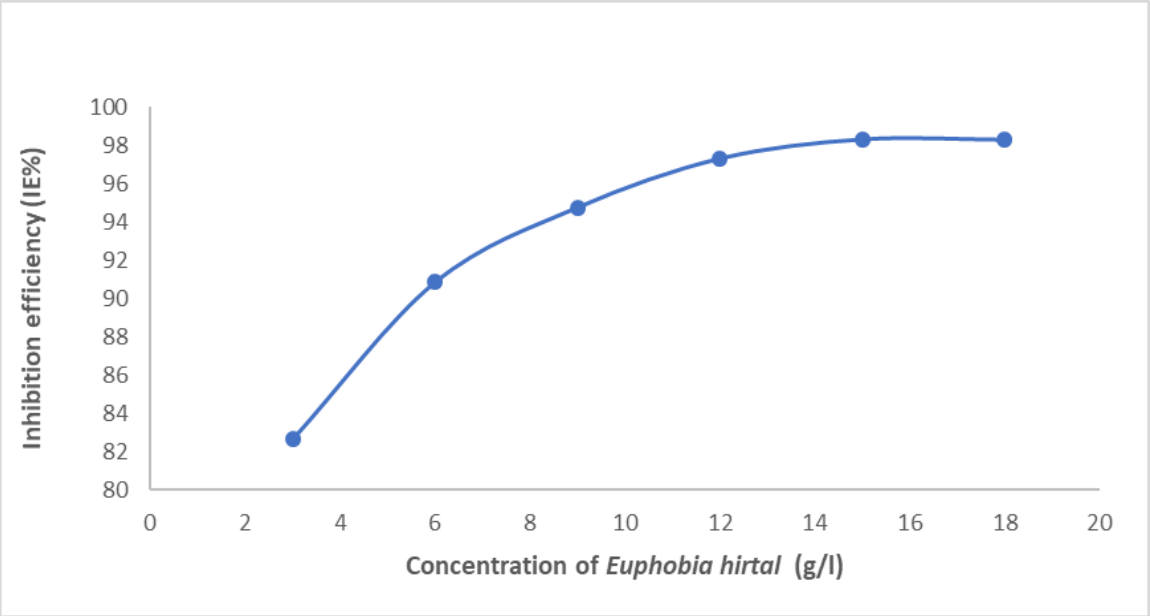

Fig. 5 – Variation of inhibition efficiency (% IE) with inhibitor concentration at 308 K.

Effect of Temperature on Inhibition Efficiency

The temperature effect on the inhibition efficiency investigated on mild steel at a range of 35–65 °C is shown in Fig. 6. The inhibition efficiency decreases with an increase in temperature. At higher temperatures, the hydrogen evolution increases on the metal surface and leads to desorption of the adsorbed inhibitor film from the metal surface as noted. It could also be attributed to an increase in the rates of ionization and diffusion of active species in the corrosion process.[22,23]

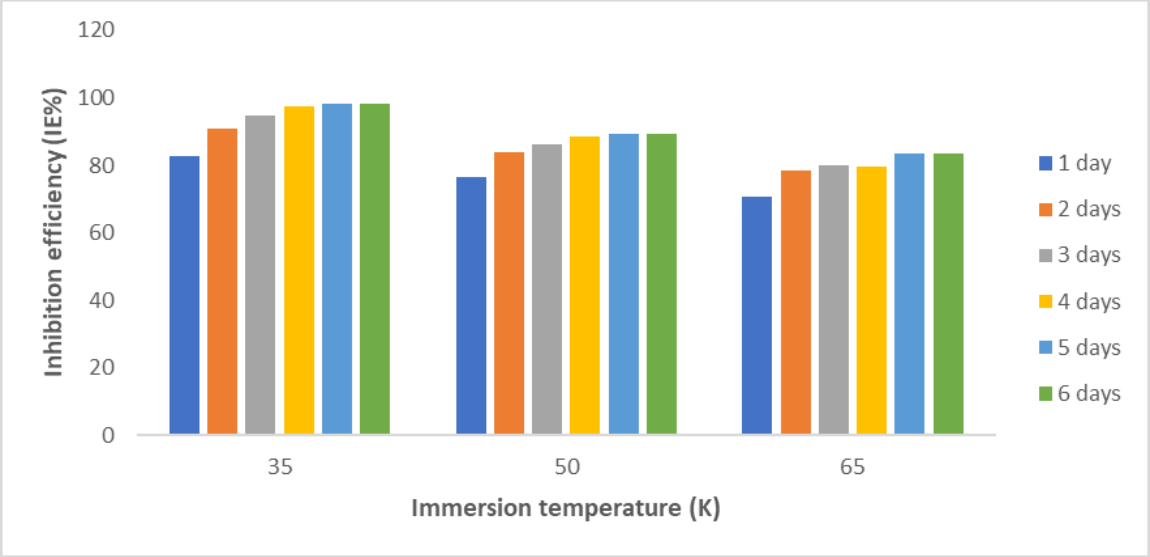

Fig. 6 – Variation of inhibition efficiency (% IE) with concentration of inhibitor at different temperatures (35–65 °C).

Potentiodynamic polarization

The potentiodynamic polarization was carried out to determine the effect of the extract of *Euphorbia hirta (EH)* inhibition of mild steel in 0.5 M hydrochloric acid. Figure 7 and Table 7 presented the plot of Tafel curves and the corrosion parameters of mild steel in 0.5 M HCl solution at various concentrations. The inhibition efficiency percent (IE%) was calculated using equation 2. The polarization measurement results shown in Table 7 indicate that the effect of the addition of *EH* extract on the inhibition of mild steel in

hydrochloric acid decreased the current density with an increase in inhibitor concentrations. The inhibition of both anodic and cathodic reactions was increased with an increase in *EH* extract concentrations. Inhibitor indicated that both anodic or cathodic types when corrosion potential shifted more than 85 mV of the corrosion potential absence inhibitor. From Table 7, E_{corr} shifted was less than 85 mV and can be classified as a mixed type of corrosion inhibitor.[24] The Tafel plots showed that the presence of the extract caused a decrease in both the anodic and cathodic current densities. The addition of *EH* extract to the HCl solution reduces the anodic dissolution of iron and retards the cathodic hydrogen evolution reactions and is similar to the works of.[25]

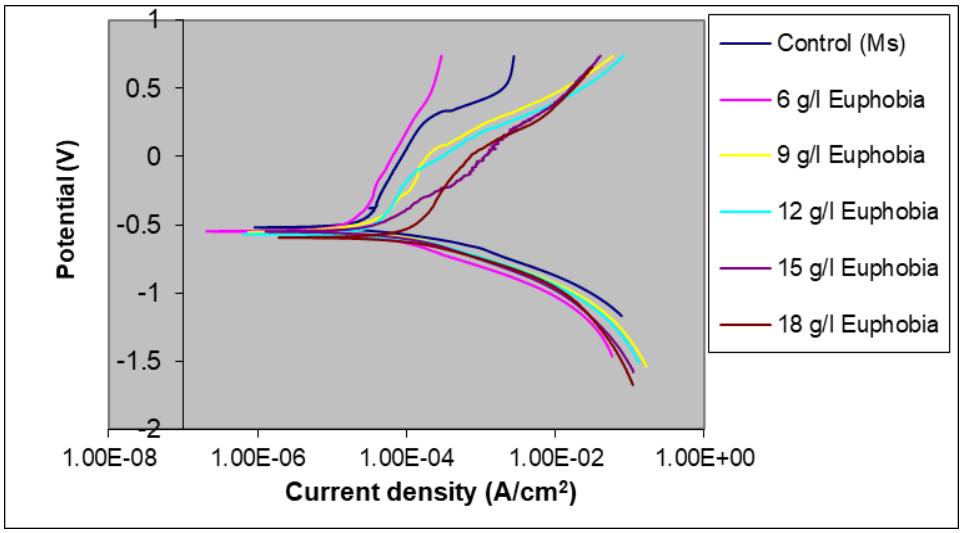

Fig. 7 – The Tafel curves for mild steel in 0.5 M HCl in the absence and presence of *EH* extract concentrations at 35 °C.

Table 7

Potentiodynamic polarization parameters of mild steel in 0.5M HCl in the absence and presence of *EH* extract at 35 °C

Concentrations (g/l)	*a* (V/Dec)	*c* (V/Dec(	E_{corr} (V/SCE)	I_{corr} (cm^2)	(%) IE
Blank (0)	100	98	–560	9.34	–
3	94	89	–540	1.990	78.69
6	94	81	–530	2.63E-01	86.77
9	90	80	–530	2.60E-02	89.98
12	86	79	–520	4.26E-04	98.36
15	86	79	–520	7.11E-06	98.33
18	82	78	–510	1.22E-07	98.29

Both corrosion current density and corrosion rate were considerably reduced in the presence of the extract. The inhibitor used was found to inhibit mild steel in the presence of HCl using the adsorption of ions and molecules on the metal surface. In this way, a protective covering was formed around the metal surface, which denies access to a corrosive environment.[26] The cathodic (βc) and anodic Tafel slopes (βa) did not change significantly with the addition of the *EH* extract. The irregularity of βa and βc proved that the *EH* extract was a mixed inhibitor that modified the mechanism of anodic dissolution and cathodic hydrogen evolution.[27,28] The optimum concentration and percentage inhibition efficiency were obtained at 12 g/l and 98.32% respectively.

Surface morphological analyses

The morphologies of mild steel samples named as received, without, and with optimum

concentrations in *Euphorbia hirta (EH)* in 0.5 M hydrochloric acid solutions were presented in Figs. 8, 9, and 10 respectively. Figure 8 presented the SEM morphology of mild steel of the as-received sample in a polished state. Figure 9 is the polished sample in the presence of 0.5 M HCl solution without extract and Fig. 10 represents the polished sample in 0.5 M HCl solution with the optimum concentration of *EH* at of 12 g/l.

The surface of the coupon in Fig. 8 was completely smooth, without any indentations except the polished surface lines that were revealed. In Fig. 9, the pits initiation commenced which is often linked to the presence of local defects at the metal surface such as flaws in the oxide or segregation of alloying elements, presence of aggressive anions such as chlorides in the environment. Pit initiation occurs on the alloy surface passivated by an oxide film due to the damage caused by passivation of the electrolyte resulting in an anodic reaction on the metal surface while the unexposed protective surrounding becomes the cathode leading to localized corrosion.[29] As time progresses, the growth of pits increases from the SEM evaluation and obviously, the corrosion resistance decreases which confirms that both weight loss and Tafel results obtained are in agreement with each other and similar to the findings.[30–32] Figure 10 coupon exposed to corrodent in the presence of optimum concentration was less rough and most of the elements present were enhanced in the presence of the extract. Hence, the propagation of pits in the coupon was impeded by the adsorption of the inhibitor on a mild steel surface. The adsorption of components of *EH* extract could be attributed to their functional groups obtained from phytoconstituents, FT-IR, and GC-MS results. The *EH* can be considered to be a good and effective corrosion inhibitor of mild steel in acid similar to the previous findings.[33–35]

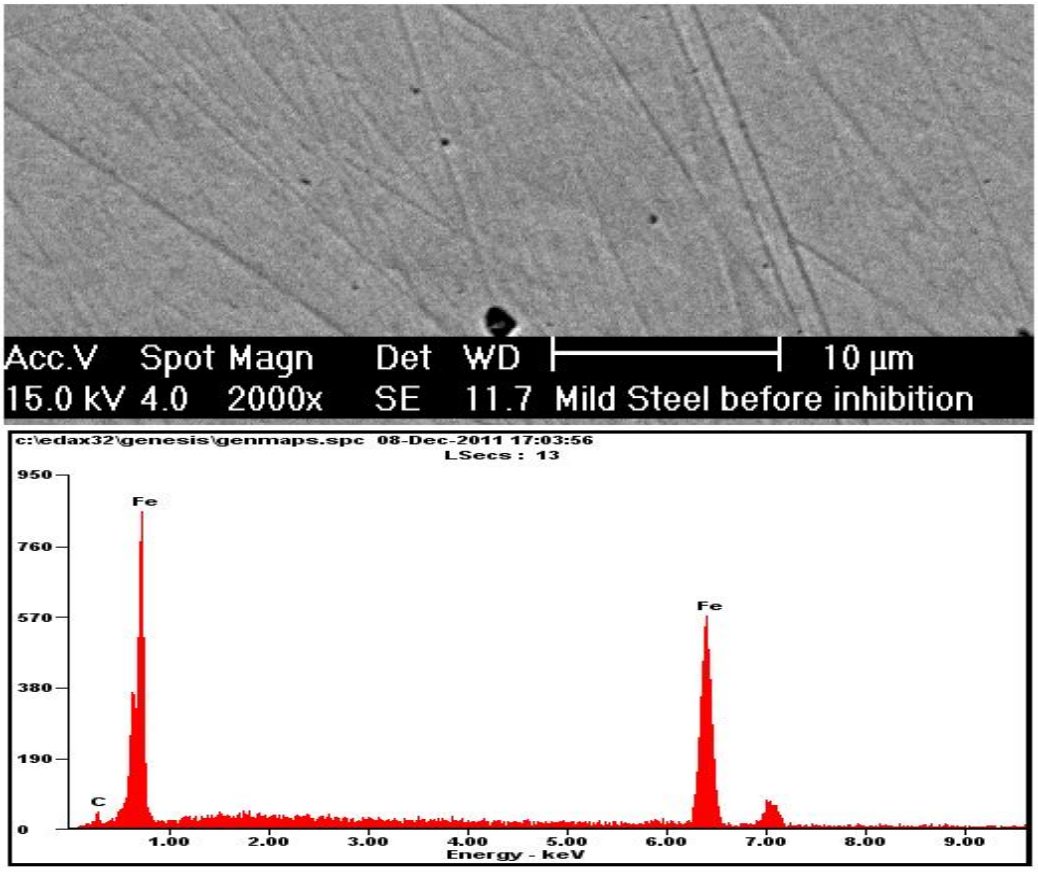

Fig. 8 – SEM/EDS of as-received mild steel.

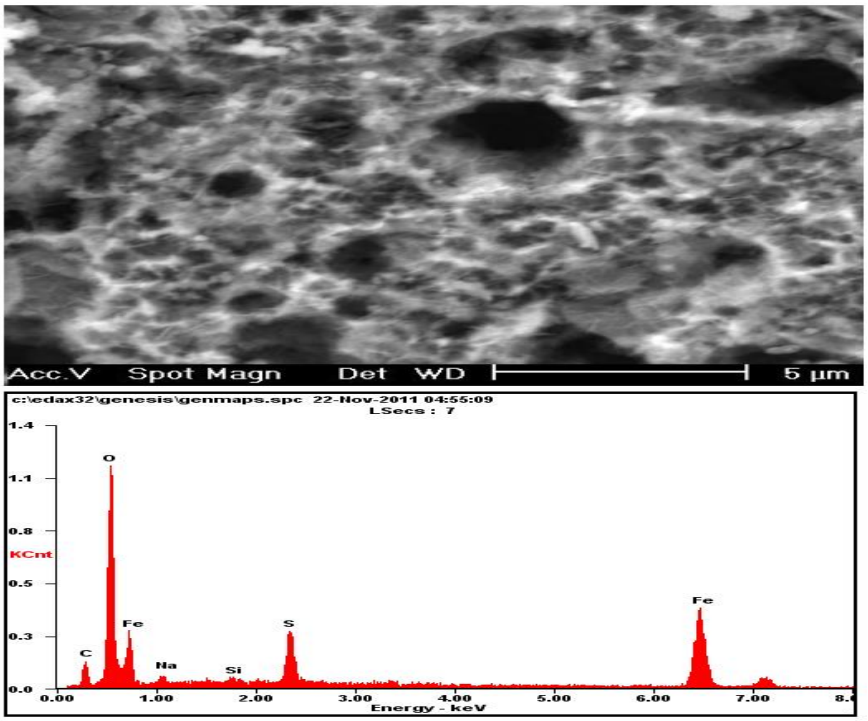

Fig. 9 – SEM/EDS of mild steel immersed in 0.5 M HCl in the absence of extract at 35 °C.

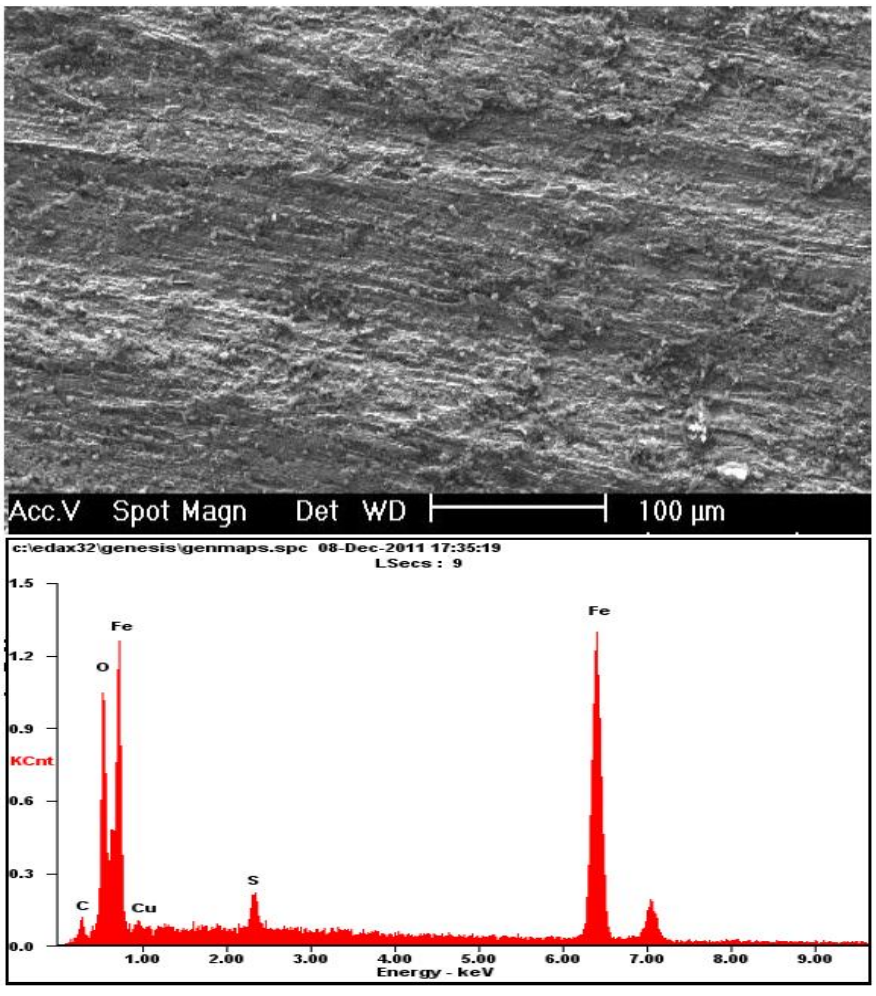

Fig. 10 – SEM/EDS of mild steel immersed in 0.5 M HCl in the presence of optimum *EH* extract at 35 °C.

CONCLUSION

From the research carried out, the following conclusion can be drawn:

Euphorbia hirta (EH) extract acted as an efficient anti-corrosive agent for mild steel in 0.5 M HCl solution. At the optimal concentration of 12 g/L, it can increase the lifespan of the mild steel by 98.32%, and this can be utilized in both oil and gas industries.

The gravimetric weight loss technique showed the inhibiting effect of *EH* with a percentage inhibition efficiency of 98.32% at 12 g/l but decreased with an increase in temperature. The Potentiodynamic polarization results showed that *Euphorbia hirta (EH)* extract acted as a mixed-type inhibitor.

The phytoconstituents, FT-IR and GC-MS revealed some major constituents such as Methyne C_nH_{2n+2} stretch, Alkyl carbonate, Primary amine, CN stretch, 9,17 Octadecadienal, 7,17 Hexadecadienal. which formed a protective thin film layer preventing the discharge of hydrogen ion (H^+) ions in the presence of an acidic solution.

The SEM/EDS morphologies of the adsorbed protective films on the mild steel surface confirmed the high performance of the inhibitive effect of the active components in *Euphorbia hirta (EH)* extract.

The results obtained using different corrosion analyses (gravimetric, potentiodynamic polarization, and electrochemical spectroscopy) are in good agreement, and therefore, the extract can be used to protect oil and gas equipment with high performance at low cost.

Acknowledgments. The authors highly appreciate and acknowledge the Africa Centre of Excellence for Sustainable Power and Energy Development, ACE-SPED, University of Nigeria, Nsukka, Energy Materials Research Group, University of Nigeria, Nsukka, Nigeria, Department of Metallurgical and Materials Engineering, University of Nigeria and Department of Chemical, Metallurgical and Materials Engineering, Tshwane University of Technology, Pretoria, South Africa.

REFERENCES

1. C. Castro-López, I. Bautista-Hernández and M. D. González-Hernández, *Molecules*, **2019**, *24*, 173-185. https://doi.org/10.3390/molecules24010173
2. R. Oukhrib, *Port Electrochim Acta.*, **2017,** *35*, 187–200.
3. M. E. S. De Jesus, *Braz. J. Dev*,**2020**, *6*, 77197–77215. https://doi.org/10.34117/bjdv6n10-227
4. M. Finšgar and J. Jackson, *Corros Sci.*, **2014**, *86*, 17–41. https://doi.org/10.1016/j.corsci.2014.04.044
5. I. Y. Suleiman and A. S Sani, *Iran. J. Sci. Technol. Trans. A Sci.*, **2018**, *42*, 1977–1987. https://doi.org/10.1007/s40995-017-0384-9
6. I. Y. Suleiman, A. Kasim, M. Z. Sirajo, A. T. Mohammed, *Rev Roum Chim.*, **2020**, *65*, 997–1007. https://doi.org/10.33224/rrch.2020.65.11.05
7. I. Y. Suleiman, *Metall Mater Eng*., **2017**, *23*, 153–166.
8. D. R. Gusti, I. Lestari, F. Farid and P. T. Sirait, *J. Phys. Conf. Ser*., **2019**, doi:10.1088/1742-6596/1282/1/012083
9. V. Vorobyova and M. E. Skiba, *S. Afr. J. Chem. Eng*., **2023**, *43*, 273–295 https://doi.org/10.1016/j.sajce.2022.11.004
10. O. Sotelo-Mazon, S. Valdez, J. Porcayo-Calderon, *Prot. Met. Phys. Chem. Surf.*, **2020**, *56*, 427–437 https://doi.org/10.1134/S2070205120020240
11. A. Singh, V. K. Singh and M. A. Quraishi, *J. Mater. Environ. Sci.*, **2010**, *1*, 162–174.
12. C. Bouyahia, *Mor. J. Chem*., **2022**, *10*, 738–751; doi.org/10.48317/IMIST.PRSM/morjchem-v10i4.32146
14. A. M. Abd Elkader, *Saudi J. Biol. Sci.*, **2022**, *29*, 1428–1433, https://doi.org/10.1016/j.sjbs.2021.11.031
18. C. Castro-López, *Molecules*, **2019**, *24*, 173. https://doi.org/10.3390/molecules24010173
19. H. Lgaz, R. Salghi, S. Jodeh and B. Hammouti, *J. Mol. Liq*., **2017**, *225*, 271–280.
20. A. M. Ayuba, M. A. Auta and N. U. Shehu, *Green Appl. Chem. J*., **2021**, *13*, 66–86; doi: 10.48419/IMIST.PRSM/rhazes-v13.28980
21. O. Id El Mouden, *Mor. J. Chem*., **2021**, *9*, 588–601. https://doi.org/10.48317/IMIST.PRSM/morjchem-v9i3.25853
22. N. J. Salazar-López, *Food Res. Inter., Part A*, **2020**, *138*, 109774, https://doi.org/10.1016/j.foodres.2020.109774
23. K. A. Kenneth, M. A. Tolulope and A. O. Peter, *J. Mater. Res. Technol*., **2014**, *3*, 9–16.
24. H. Lgaz, *J. Mol. Liq*., **2017**, 225, 271–280. https :// doi.org/10.1016/j.molli q.2016.11.039
25. M. S. Al-Otaibi, *Arab. J. Chem*., **2014**, *7*, 340–346
26. A. Ghazoui, N. Benchat, F. El-Hajjaji, M. Taleb, Z. Rais and R. Saddik, *J. Alloys Compd.*, **2017**, *693*, 510–517.
27. F. El Hajjaji, H. Greche, M. Taleb, A. Chetouani, A. Aouniti and B. Hammouti, *J. Mater. Environ. Sci*., **2016**, *7*, 567–578.
28. O. Benali, C. Selles and R. Salghi, *Res. Chem. Intermediat*., **2014**, *40*, 259–268.
29. A. S. Fouda, M. A. Ismail, G. Y. Elewady and A. S. Abousalem, *J. Mol. Liq.*, **2017**, *240*, 372–388.
30. A. H. Al-Moubaraki, A. Al-Judaibi, A. Maryam, *Int. J. Electrochem. Sci*., **2015**, *10*, 4252– 4278
31. M. Yadav, K. Gope, N. Kumari and P. Yadav, *J. Mol. Liq.*, **2016**, *216*, 78–86.
32. K. R. Ansari, M. A. Quraishi and A. Singh, *J. Ind. Eng. Chem*., **2015**, *25*, 89–98.
33. M. Babutzka, A. Heyn and P. Rosemann, *Maters Corros.*, **2018**, *24*, 1–12.
34. N. Chaubey, D. K. Yadav, V. K. Singh and M. Quraishi, *Ain Shams Eng. J.*, **2017**, *8*, 673–682.
35. R. T. Olorunmota, *J. Adv. Biol. Biotechnol*., **2017,** *16*, 1–9.